Deep-UV Laser-Based Fluorescence Lifetime Imaging Microscopy of Single Molecules

Qiang Li, Thomas Ruckstuhl, and Stefan Seeger*

Physikalisch-Chemisches Institut der Universität Zürich, Winterthurerstrasse 190, CH-8057 Zürich, Switzerland

Received: November 18, 2003; In Final Form: February 25, 2004

Deep ultraviolet (deep-UV) laser-based fluorescence lifetime imaging microscopy of single dye molecules adsorbed on quartz glass surfaces is presented. The instrumental setup uses a mode-locked diode-pumped picosecond laser emitting at 266 nm with a repetition rate of 40 MHz. Applying the time-resolved single-photon counting method, we investigated the laser dye 2,2‴-dimethyl-*p*-quaterphenyl and obtained the fluorescence intensity and fluorescence lifetime images of individual adsorbed molecules. The described setup is also well-suited for biological applications for ultrasensitive detection of intrinsic fluorescence after UV excitation.

Introduction

Fluorescence spectroscopy has been successfully used to detect single molecules at room temperature in solution or at interfaces with preferable signal-to-noise ratios. In particular, single molecule detection at surfaces is of interest for application in life science.[1−5] To suppress scattered light, the most common way is to use a small detection volume through the use of a confocal epifluorescence microscope or supercritical angle fluorescence/total internal reflection fluorescence (SAF/TIRF) and spectral filters by taking advantage of the frequency shift of the fluorescence emission with respect to the laser excitation (Stocks shift). So far, dyes have been used for ultrasensitive detection and identification by one-photon excitation in a wavelength region from green to near-IR.[6−9] Recently, Brand et al.[10] reported single molecule identification of Coumarin-120 in solution via one-photon excitation in the near-UV (350 nm) and two-photon excitation at 700 nm. To the best of our knowledge, single dye molecules with an absorption maximum in the deep UV have not been detected by one-photon excitation. The major drawbacks for the native fluorescence detection approach after excitation with UV light have been the limitations of short-pulse-duration solid-state UV excitation sources and the lack of suitable quartz microscope lenses, which must be chromatically corrected and transparent for both absorption and emission wavelengths. The suppression of background signal due to Rayleigh scattering, which increases with the fourth power of the UV excitation laser frequency, has also inhibited this approach.

Steady-state and time-resolved fluorescence measurements are widely used in analytical and bioanalytical applications. However, time-resolved fluorescence detection delivers more information than steady-state experiments. Furthermore, steady-state systems suffer from problems such as photobleaching, probe concentration variation, and scattering artifacts. Time-resolved fluorescence microscopy (TRFM) is much less sensitive to those effects.[11,12] TRFM enables mapping of fluorescence lifetimes, which is vital for the determination of the spatial orientation of probe molecules. Furthermore, it is used to distinguish between fluorescence dyes that have similar spectral characteristics, and it provides a means of discriminating against background fluorescence.[13] Two time-resolved fluorescence detection methods are in widespread use for fluorescence lifetime imaging (FLIM): the frequency-domain and time-domain methods.[11] The main advantage of time-domain measurements is that sub-nanosecond gated fluorescence images are obtained directly with sufficient signal intensity in real time. Instruments for time-domain FLIM measurements based on gating the fluorescence signal, using either time-correlated single-photon counting (TCSPC) techniques[14−16] or gated image intensifiers,[17−19] have been reported. Currently, almost all time-domain measurements are performed using TCSPC, because of the technical improvements in laser light sources, photodetector sensitivity, and objective optics. In TCSPC, the time lag between an excitation laser pulse and the emission of a fluorescence photon is measured for many individual photons. Combination of these time lags into a histogram and subsequent fitting of the histogram with an exponential decay allows for accurate determination of the fluorescence lifetime. Recently, ultrasensitive fluorescence detection at the single-molecule level on surfaces has been reported based on a pulsed visible laser using the TCSPC technique.[20−25]

The autofluorescence of biological samples results from the intrinsic fluorescence of proteins, co-enzymes, and other components of body fluids. In proteins, the three aromatic amino acid residues—tryptophan, tyrosine, and phenylalanine—may contribute to their intrinsic fluorescence when excited in the UV region of 260−280 nm.[11] In the past year, single protein molecule detection has relied on the use of a large variety of highly efficient fluorescent labels in the visible spectral range. Although the use of fluorescent tags greatly improve the sensitivity, they can suffer from a lack of specificity for the analytes and can change the reaction kinetics or induce incomplete reactions when conformational dynamics are studied. In particular, this is the case if the dynamic components of the biomolecule have a size similar to that of the attached dye. In such situations, the possibility of using the native fluorescence of the dynamical component is a considerable improvement. Recently, the intrinsic fluorescence emission of biomolecules has been utilized in some research groups for detection.[26−28] Lippitz et al.[28] reported results on two-photon excitation microscopy of avidin-coated spheres, using intrinsic tryptophan

* Author to whom correspondence should be addressed. Fax: +41-1-6356813. E-mail: sseeger@pci.unizh.ch.

10.1021/jp0375160 CCC: $27.50
Published on Web 05/11/2004

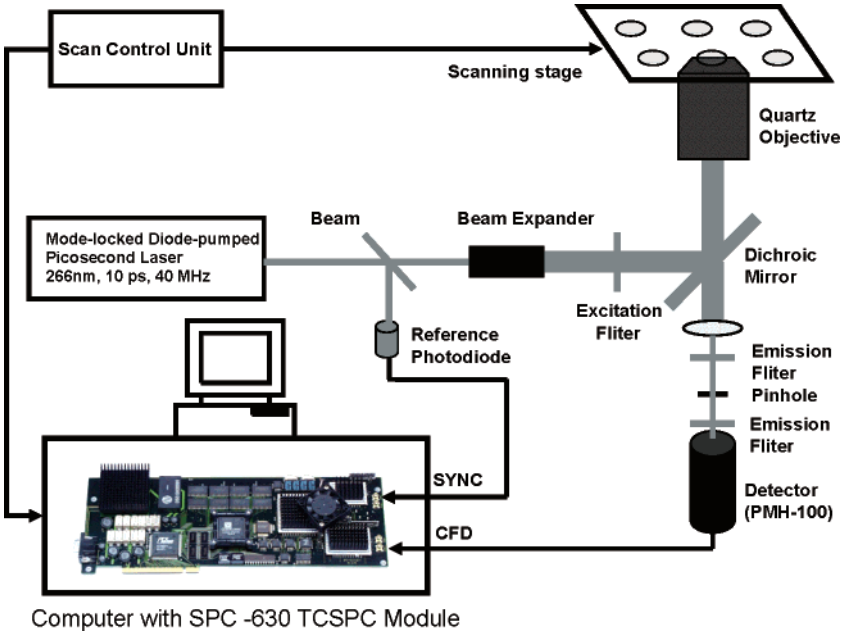

Figure 1. Setup for the deep-UV laser-based fluorescence lifetime imaging microscopy (FLIM) system.

(Trp) emission. They suggest that, under favorable conditions, Trp-containing biomolecules can be investigated at the single-molecule level without introducing artificial dye labels. Until now, there has been no report on single-molecule detection of Trp or proteins containing Trp by means of their intrinsic fluorescence emission after one-photon excitation. The major problem is the weak photostability of Trp molecules.

In this paper, we present a deep UV−FLIM system based on a mode-locked diode-pumped picosecond deep-UV laser using the TCSPC method. To demonstrate the lifetime imaging capabilities on the single-molecule level, a UV laser dye adsorbed on quartz glass surface was used for test samples. We obtained fluorescence intensity and lifetime images of single dye molecules on glass substrates using a pulsed UV laser emitting at 266 nm with a repetition rate of 40 MHz as an excitation source, in combination with an *x*,*y*-scanning microscope. The primarily purpose of this system is its use for UV native fluorescence detection of biological macromolecules.

Experimental Section

The experimental setup for confocal fluorescence lifetime imaging microscopy is shown in Figure 1. It consists of a 266-nm UV mode-locked diode-pumped picosecond laser (model GE-100-XHP-FHG, Time-Bandwidth Products, Inc., Switzerland). The laser system provides pulses with a duration of <10 ps and a repetition rate of 40 MHz; the laser has a maximum power output of 20 mW. The polarized laser beam was split 50/50 by a beam splitter (Laser Components GmbH, Germany), sending 50% into a high-speed photodiode module (Becker & Hickl GmbH, Berlin, Germany), which is used for triggering of the TCSPC module. The second beam passed an excitation filter (model 254WB25, Omega Optical) and is directed into the quartz microscope objective (40×, NA = 0.80, Partec GmbH, Münster, Germany) by a dichroic beam splitter (model 290DCLP, Omega Optical). The laser power was adjusted by inserting different neutral density filters (Melles Griot). Surface scans were performed by moving the sample with a motorized *x*,*y*-translation stage (Märzhäuser, Wetzlar, Germany). The fluorescence light was collected by the same objective and transmitted through the dichroic mirror. A lens (focal distance of 200 mm) focuses the light onto a pinhole for confocal imaging. After the pinhole, the fluorescence emission is detected by a high-speed photomultiplier tube (PMT) detector head (model PMH-100-6, Becker & Hickl GmbH). Two emission band-pass filters (model 330WB60, Omega Optical)—one positioned directly after the lens, and the other positioned directly in front of the detector—discriminate fluorescence against scattered light. The signal pulses of the PMT was fed into a TCSPC PC interface card (model SPC-630, Becker & Hickl GmbH) to acquire time-resolved data. The TCSPC was performed in the reversed mode, i.e., the signal of the PMT was used to start the clock of the time-to-amplitude converter and the reference signal of the laser from the high-speed photodiode was used as the stop signal. Software written in C++ was developed for synchronization of the scanning motion with the data acquisition. The instrument response function (IRF) was measured by replacing the sample with a scattering dispersion of colloidal silicon dioxide (SiO_2) particles in water (particle size of 11 nm), and then recording the Rayleigh scattering of the excitation light without two emission filters. With this setup, an IRF of 240 ps (full width at half maximum, fwhm) was measured. The fluorescence decay time constants were obtained by deconvoluting the IRF.

In all experiments reported below, the scan driver was set to perform 500 scan steps in each direction, with a step size of 160 nm and a step time of 2 ms. The fluorescence intensity image was calculated by sorting the detected photons into time bins with a bin width of 2 ms, and ordering the time bins into a 500 × 500 array. The fluorescence lifetime image can be calculated using the TCSPC times of the photons, because the exact correlation between detected photons and image position is known. According to ref 22, the lifetime of an image pixel was simply calculated as the average lifetime of all the photons falling into that pixel.

The fluorescence dye, 2,2‴-dimethyl-*p*-quaterphenyl (BMQ), was purchased from Lambda Physik without further purification. All experiments were conducted at room temperature. Stock solutions of the dye (1×10^{-4} mol/L) in cyclohexane (spectrophotometric grade, Fluka) were stored at −20 °C until use. To adjust the dye concentration we used the UV/VIS/NIR

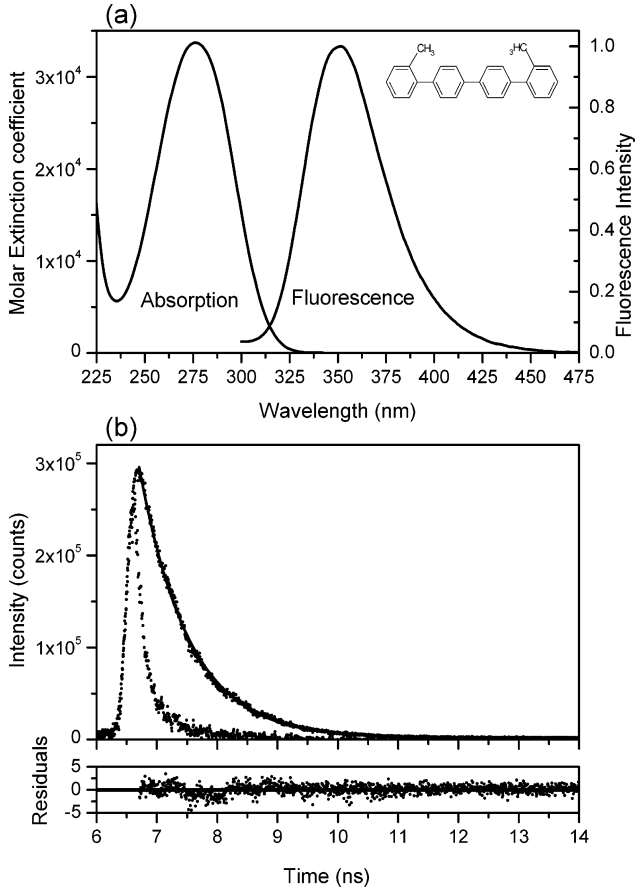

Figure 2. (a) Absorption and fluorescence emission spectra of BMQ in cyclohexane bulk solution. Fluorescence emission was excited at 266 nm with 1×10^{-8} mol/L solution of BMQ. Inset shows the molecular structure of BMQ dye. (b) Time-resolved fluorescence decay of BMQ in cyclohexane excited at 266 nm, together with the instrument response function (IRF). Corresponding fit revealed a monoexponential fluorescence lifetime of 0.79 ns with a reduced χ^2 value of 0.85. The weighted residuals of the fit are also shown in the lower panel.

spectroscopy (model Lambda 900, Perkin−Elmer). Steady-state fluorescence spectra were measured in standard quartz cuvettes with a luminescence spectrometer (model LS 50B, Perkin−Elmer). Time-resolved data of bulk solutions were measured at a concentration of 1×10^{-8} mol/L. Sample preparation was done by spin-coating BMQ cyclohexane solution with different concentrations (1×10^{-8}−1×10^{-11} mol/L at 2000 rpm) onto clean quartz cover slides (170 μm thick, SPI Supplies); using this methodology, the molecules are immobilized on a glass/air interface. Prior to use, the quartz cover slides were cleaned for 60 min in $CHCl_3$ in an ultrasonic bath, followed by washing with doubled distilled water and then dried in nitrogen flow. After spin coating, the samples were immediately scanned under ambient conditions with a FLIM system.

Results and Discussion

2,2‴-Dimethyl-*p*-quaterphenyl (BMQ) is a commercially available UV laser dye with high photochemical stability.[29,30] The UV absorption and fluorescence emission spectra of BMQ in cyclohexane are shown in Figure 2a. The maximum absorption of BMQ is observed at 275 nm, with an extinction coefficient (ϵ) of 3.37×10^4 L mol^{-1} cm^{-1}, and the fluorescence quantum yield of BMQ dye in ethanol is 0.71.[29] In addition to the high quantum efficiency, the dye has the advantage of being excitable with UV laser emitting at 266 nm ($\epsilon_{266\text{nm}} = 2.99 \times 10^4$ L mol^{-1} cm^{-1}). The UV absorption and fluorescence emission spectra of BMQ in cyclohexane are very similar to the spectra in ethanol.[29] Compared to the dyes excited in the visible region of the spectrum (for example, rhodamines), BMQ has a large Stokes shift of 85 nm. This allows a good spectral separation of the fluorescence emission from Raman scattering, resulting in a low background level. Therefore, BMQ is a good candidate for single-molecule detection. Figure 2b shows the fluorescence decay of BMQ in bulk cyclohexane solution, together with the instrument response function (IRF). A low concentration of 1×10^{-8} mol/L was used in these experiments in order to avoid energy homotransfer between BMQ molecules. The decay parameters were determined by least-squares deconvolution, and their quality was judged by the reduced χ^2 value and the randomness of the weighted residuals. As can be observed from the residuals, the largest error occurs at the beginning of the fit. The molecule shows a single-exponential decay with a lifetime of 0.79 ns and a χ^2 value of 0.85; the lifetime of BMQ in bulk cyclohexane is in good agreement with the value measured in ethanol at room temperature.[30]

Spin coating has been widely used in preparation of samples for the detection of single molecules absorbed on a glass surface.[24,25,31−34] One prepares the sample by spin-coating a solution of dye molecules onto a glass surface. After the solvent has evaporated, individual molecules are immobilized on the surface, the distance between molecules is adjusted by the concentration of dye molecules in the solution and spin-coating parameters. To determine the BMQ concentration at which isolated single molecules are immobilized on the quartz glass surface, the sample were prepared by spin coating at different concentrations of the BMQ dye solution (1×10^{-8}−1×10^{-11} mol/L) onto a quartz glass surface. Figure 3a−c show fluorescence images at difference molecular densities. The maximum of photon counts exhibits similar values for each sample after spin-coating solutions of BMQ concentrations of $<5 \times 10^{-10}$ mol/L, whereas above this concentration the maximum number of photons increases as the BMQ concentration increases. The spot size also becomes larger at concentrations of $>5 \times 10^{-10}$ mol/L. The increase in brightness and the size of the spots implies that BMQ molecules aggregate on the surface (see Figure 3a). In addition, we also measured the average number of photons per spot for different concentrations (see Figure 3d). An increase in the number of photons per spot at concentrations $>5 \times 10^{-10}$ mol/L has been observed; however, no concentration dependence of the number of photons at concentrations of 1×10^{-10} mol/L and less is observed. We attribute the bright spots in the images of Figures 3b and 3c to the fluorescence from single BMQ dye molecules.

To get more evidence of single-molecule detection, we repeatedly scanned one line on the sample that was prepared by spin-coating 5×10^{-10} mol/L of BMQ solution. This allowed us to obtain the fluorescence intensity of one or several single molecules over a long time scale. Figure 4 shows two such intensity-versus-time traces of different BMQ dye molecules; only two levels of intensity (fluorescence and background) are observed. This is one of the typical features of single-dye emitters; it is called one-step photobleaching behavior. The transition from emissive to nonemissive states and the final cessation of emission due to irreversible photobleaching are observed.

To demonstrate the principle of the confocal FLIM of single molecules in the deep-UV region further, a BMQ solution (concentration of 5×10^{-10} mol/L) was adsorbed on quartz cover slides by spin coating. Figure 5a shows scanning confocal

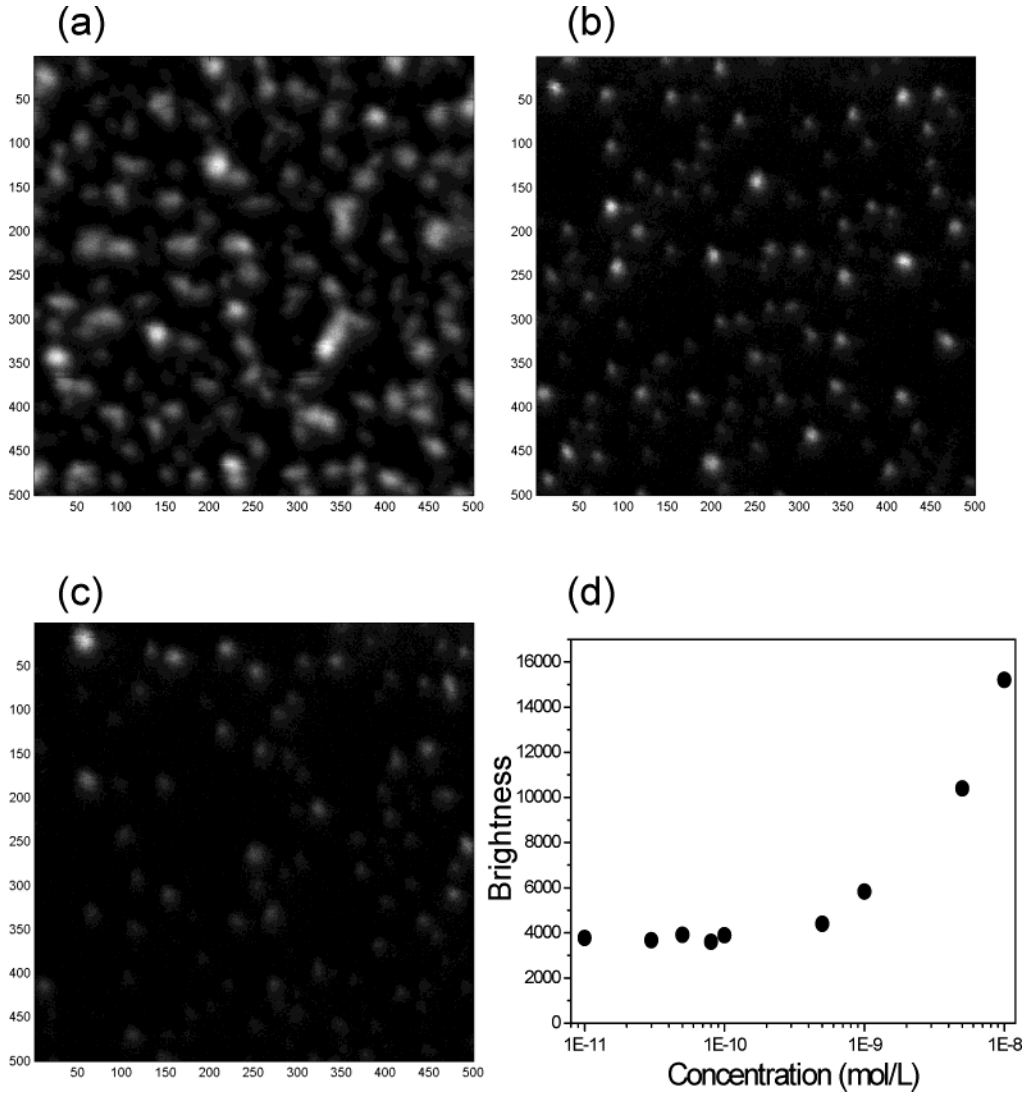

Figure 3. Fluorescence intensity images of dispersed BMQ dye molecules spin-coated from cyclohexane solutions with concentrations of (a) 1×10^{-8}, (b) 1×10^{-10}, and (c) 1×10^{-11} mol/L. Panel d shows the dependence of the average number of photons per spot on concentrations of the BMQ solution. Below concentrations of $\sim 5 \times 10^{-10}$ mol/L, the fluorescence from individual dye molecules can be spatially resolved.

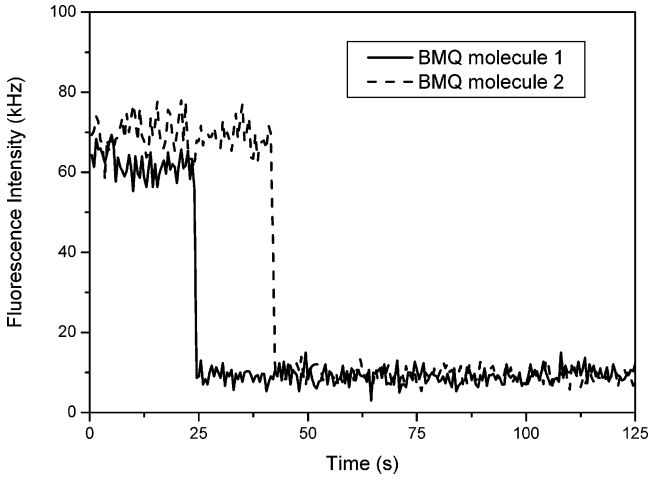

Figure 4. Time traces of the fluorescence intensity of BMQ molecules. Although the laser is focused on different molecules, one-step photobleaching of BMQ is observed. The BMQ cyclohexane solution used for spin coating had a concentration of 5×10^{-10} mol/L.

fluorescence intensity images of BMQ molecules. The images exhibit clearly circular fluorescing spots with a count rate of up to 85 kHz. With a background count rate of 12 kHz, signal-to-noise ratios of up to 7 were calculated for the most pixels in our experiments. The fluorescence lifetime image shown in Figure 5b was calculated by averaging the TCSPC times of all detected photons that fall into that pixel. To suppress the background efficiently, pixels corresponding to count rates of <12 kHz were excluded. The resulting lifetime image shows the fluorescence lifetime of BMQ molecules of ~ 1 ns. For further analysis, we calculated the spot-integrated fluorescence lifetime of >200 BMQ molecules spots by adding up all photon counts collected per single dye molecule. Figure 5c shows the fluorescence lifetime distribution of single BMQ molecules adsorbed on a glass surface, the obtained distribution of fluorescence lifetime fits a Gaussian function well. The measured lifetime is 1.06 ± 0.14 ns, which is longer than that measured in bulk solution. The fluorescence lifetime of single molecules absorbed on the surface is strongly influenced by its local environment; the distribution of the fluorescence lifetimes is controlled by the orientation of the emission dipole, the distance from the interface, and the refractive index difference at the dielectric interface.[33,34] Macklin et al.[34] investigated the variation in the excited-state lifetime of single molecules located on a polymer/air interface plane by far-field microscopy. They attributed greater variations in the lifetime to different out-of-

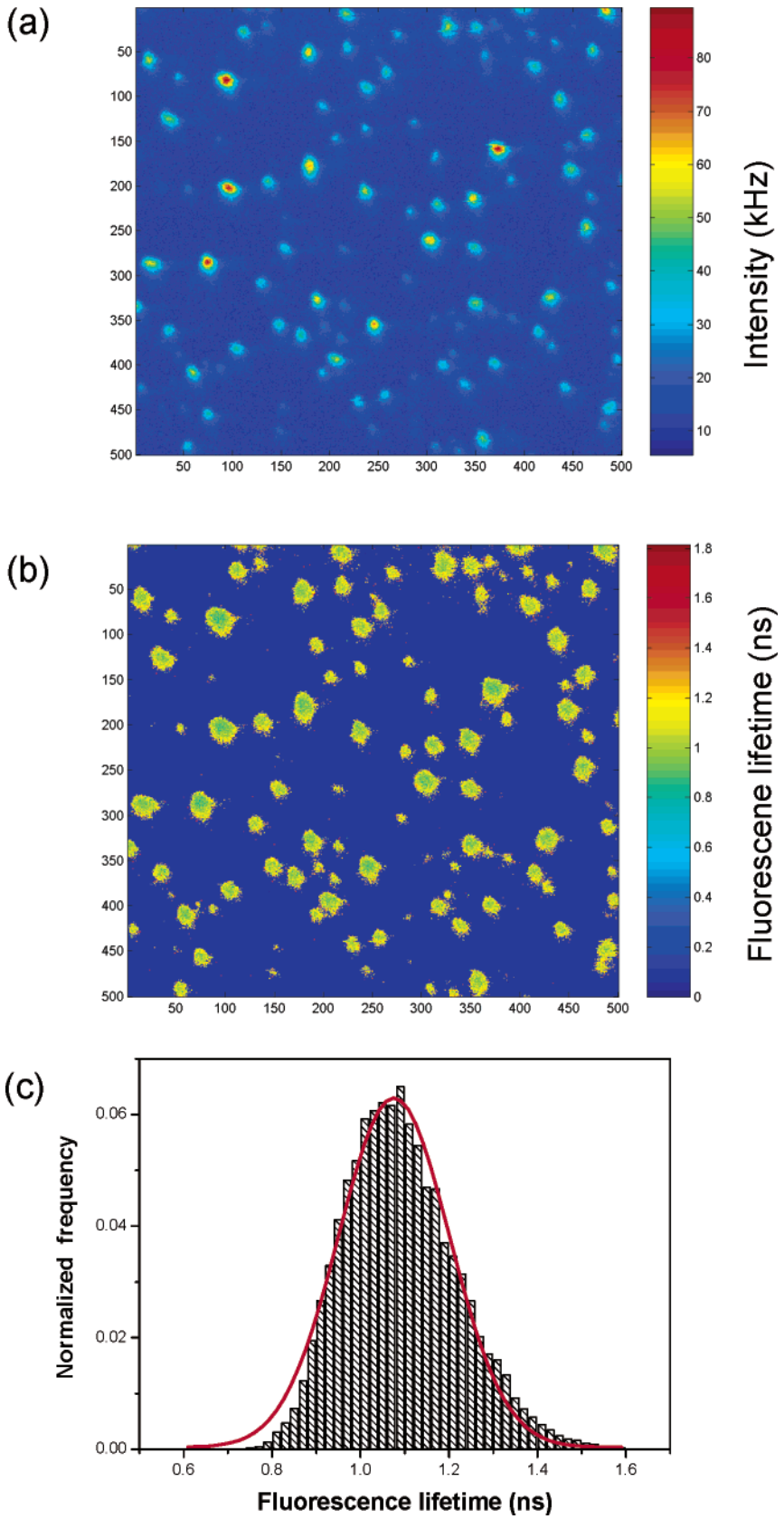

Figure 5. (a) Fluorescence intensity and (b) fluorescence lifetime images of single BMQ dye molecules adsorbed on a quartz glass surface, using a 5×10^{-11} mol/L solution of BMQ for spin coating. Single molecules are clearly visible as circular fluorescing spots. Pixels corresponding to count rates of <12 kHz were excluded in fluorescence lifetime imaging. (c) Histogram of determined fluorescence lifetime of single BMQ molecules on a surface obtained from an integrated fluorescence lifetime of >200 molecules. Corresponding Gaussian distribution fit yields the average lifetime of 1.06 ± 0.14 ns.

plane orientation of the molecular dipoles with respect to the interface. The orientation of molecules and emission dipole can be estimated using the fluorescence rate and fluorescence lifetime. In the experiment described in this publication, the

lifetime distribution measured for single BMQ molecules is relatively narrow and homogeneous, which indicates that most molecules have a similar environment, i.e., take a more or less pronounced planar orientation with similar orientations of the emission dipoles on the glass surface.

Conclusion

We have demonstrated single-molecule detection in the deep-UV region after one-photon excitation for the first time. This was achieved by time-correlated single-photon counting (TCSPC) microscopy, using a pulsed mode-locked diode-pumped UV laser. The fluorescence lifetime distributions of single 2,2‴-dimethyl-*p*-quaterphenyl (BMQ) dye molecules reflect the distribution of the transition dipoles on the surface, and our results suggest that most molecules have similar orientations of the emission dipoles on the glass surface. Because a large number of biological species have intrinsic fluorescence when excited in the UV region, UV laser excitation will be an attractive alternative to derivatizing these compounds with fluorescence labels excited at the visible region. Hence, our UV laser-based fluorescence lifetime imaging microscopy is ideally suited for the identification of biological macromolecules on ultrasensitive detection, using intrinsic fluorescence at UV excitation. We are currently working on exploring the potential of native fluorescence detection of proteins containing a large number of tryptophans.

Acknowledgment. This work was supported by the Swiss National Science Foundation.

References and Notes

(1) Löscher, F.; Ruckstuhl, T.; Seeger, S. *Adv. Mater.* **1998**, *10*, 1005.
(2) Löscher, F.; Böhme, S.; Martin, J.; Seeger, S. *Anal. Chem.* **1998**, *70*, 3202.
(3) Ruckstuhl, T.; Enderlein, J.; Jung, S.; Seeger, S. *Anal. Chem.* **2000**, *72*, 2117.
(4) Ruckstuhl, T.; Seeger, S. *Appl. Opt.* **2003**, *42*, 3277.
(5) Laib, S.; Rankl, M.; Ruckstuhl, T.; Seeger, S. *Nucleic Acids Res.* **2003**, *31*, e138
(6) Nie, S.; Chiu, D. T.; Zare, R. N. *Anal. Chem.* **1995**, *67*, 2849.
(7) Lee, Y. H.; Maus, G. R.; Smith, B. W.; Wineforder, J. D. *Anal. Chem.* **1994**, *66*, 4142.
(8) Soper, S. A.; Mattingly, Q. L.; Vegunta, P. *Anal. Chem.* **1993**, *65*, 740.
(9) Müller, R.; Zander, C.; Sauer, M.; Deimel, M.; Ko, D. S.; Siebert, S.; Arden-Jacbo, J.; Deltau, G.; Marx, N. J.; Drexhage, K. H.; Wolfrum, J. *Chem. Phys. Lett.* **1996**, *262*, 716.
(10) Brand, L.; Eggeling, C.; Zander, C.; Drexhage, K. H.; Seidel, C. A. M. *J. Phys. Chem. A* **1997**, *101*, 4313.
(11) Lakowicz, J. R. *Principles of Fluorescence Spectroscopy*, 2nd ed.; Plenum Press: New York, 1999.
(12) Lakowicz, J. R. *Topics in Fluorescence Spectroscopy*, *Vol. 1: Techniques*; Plenum Press: New York, 1992.
(13) Seeger, S.; Bachteler, G.; Drexhage, K. H.; Deltau, G.; Arden-Jacob, J.; Galla, K.; Han, K. T.; Müller, R.; Köllner, M.; Rumphorst, A.; Sauer, M.; Schulz, A.; Wolfrum, J. *Ber. Bunsen.—Phys. Chem.* **1993**, *97*, 1542.
(14) Gerritsen, H. C.; Sanders, R.; Draaijer, A. *Proc. SPIE* **1994**, *2329*, 260.
(15) Sanders, R.; Gerritsen, H. C.; Draaijer, A.; Houpt, P. M.; van Veen, J. J. F.; Levine, Y. K. *Proc. SPIE* **1994**, *2137*, 56.
(16) Ghiggino, K. P.; Harris, M. R.; Spizzirri, P. G. *Rev. Sci. Instrum.* **1992**, *63*, 2999.
(17) Young, P. E.; Hares, J. D.; Kilkenny, J. D.; Phillion, D. W.; Campbell, E. M. *Rev. Sci. Instrum.* **1988**, *59*, 1457.
(18) Wang, X. F.; Periasamy, A.; Gordon, G. W.; Wodnicki, P.; Herman, B. *Proc. SPIE* **1994**, *2137*, 64.
(19) Sytsma, J.; Vroom, J. M.; Grauw, C. J.; Gerritsen, H. C. *J. Microsc.* **1998**, *191*, 39.
(20) Tinnefeld, P.; Buschmann, V.; Herten, D. P.; Han, K. T.; Sauer, M. *Single Mol.* **2000**, *1*, 215.
(21) Heilemann, M.; Herten, D. P.; Heintzmann, R.; Cremer, C.; Müller, C.; Tinnefeld, P.; Weston, K. D.; Wolfrum, J.; Sauer, M. *Anal. Chem.* **2002**, *74*, 3511.
(22) Böhmer, M.; Pampaloni, F.; Wahl, M.; Rahn, H. J.; Erdmann, R.; Enderlein, J. *Rev. Sci. Instrum.* **2001**, *72*, 4145.
(23) Trabesinger, W.; Hübner, C. G.; Hecht, B.; Wild, U. P. *Rev. Sci. Instrum.* **2002**, *73*, 3122.
(24) Weston, K. D.; Carson, P. J.; Metiu, H.; Buratto, S. K. *J. Chem. Phys.* **1998**, *109*, 7474.
(25) Sànchez, E. J.; Novotny, L.; Holtom, G. R.; Xie, X. S. *J. Phys. Chem. A* **1997**, *101*, 7019.
(26) Dickson, R. M.; Cubitt, A. B.; Tsien, R. Y.; Moerner, W. E. *Nature* **1997**, *388*, 355.
(27) Wennmalm, S.; Blom, H.; Wellerman, L.; Rigler, R. *Biol. Chem.* **2001**, *382*, 393.
(28) Lippitz, M.; Erker, W.; Decker, H.; van Holde, K. E.; Basché, T. *Proc. Natl. Acad. Sci. U.S.A.* **2002**, *99*, 2772.
(29) Güsten, H.; Rinke, M.; Wirth, H. O. *Appl. Phys. B* **1988**, *45*, 279.
(30) Rinke, M.; Güsten, H.; Ache, H. J. *J. Phys. Chem.* **1986**, *90*, 2661.
(31) Hernando, J.; van der Schaaf, M.; van Dijk, E. M. H. P.; Sauer, M.; Gercía-Parajó, M. F.; van Hulst, N. F. *J Phys. Chem. A* **2003**, *107*, 43.
(32) Vallée, R.; Tomczak, N.; Gersen, H.; van Dijk, E. M. H. P.; Gercía-Parajó, M. F.; Vancso, G. J.; van Hulst, N. F. *Chem Phys. Lett.* **2001**, *348*, 161.
(33) Kreiter, M.; Prummer, M.; Hecht, B.; Wild, U. P. *J. Chem. Phys.* **2002**, *117*, 9430.
(34) Macklin, J. J.; Trautman, J. K.; Harris, T. D.; Brus, L. E. *Science* **1996**, *272*, 255.